2026 11th IEEE RAS/EMBS International Conference for
Biomedical Robotics and Biomechatronics (BioRob)
August 1-4 2026. Edmonton, Canada

2026 11th IEEE RAS/EMBS International Conference on Biomedical Robotics and Biomechatronics (BioRob) | 979-8-3315-4813-1/26/$31.00 ©2026 IEEE | DOI: 10.1109/BIOROB66782.2026.11681058

Embedded Multimodal Textile Actuator for Mechanotherapy: a Proof-of-Concept Study

Marco Lupi[1], Sophie Skach[1], Jiří Navrátil[2], Maija Vaara[3], Pedro Silva[3], Jacopo Quaglierini[1], Radek Soukup[2], Jaana Vapaavuori[3], Leonardo Cappello[1], *Senior Member*

***Abstract*— Home-based rehabilitation is increasingly recognised as a key strategy for providing continuous, accessible and cost-effective therapies while reducing dependence on specialised equipment and clinical supervision. This is particularly relevant for musculoskeletal and post-surgical rehabilitation. Extending functional therapies (e.g., mechanotherapy and heat therapy) to wearable platforms requires compact, lightweight devices that preserve therapeutic efficacy outside of clinical settings. This work presents the concept and preliminary investigation of a fully textile, programmable compression module that integrates localised heating into a lightweight, compact architecture. The system employs thermally activated twisted and coiled polymer actuators (TATCPAs) for controlled compression and embroidered hybrid resistive elements for efficient heating, synergistically combining mechanotherapy and heat therapy in a single wearable device for the first time. This proof-of-concept consists of a single compact drive module, intended as the basic building block to devise a fully functional wearable system. This approach provides a scalable basis for extending rehabilitation beyond clinical settings, facilitating accessible home-based therapy.**

Keywords—mechanotherapy, shape-memory polymers, textile electronics, textile robotics, multimodal actuation, wearable robotics, heat therapy

I. INTRODUCTION

Musculoskeletal (MSK) disorders, which encompass a broad spectrum of conditions affecting joints, muscles, tendons, and bones, represent one of the leading causes of pain, disability, and reduced quality of life worldwide [1]. The World Health Organization estimated in December 2024 that over 1.7 billion people worldwide are affected by MSK conditions. These conditions account for nearly one third of general practice consultations and represent a major cause of work absences, substantially impacting healthcare systems and economic productivity [2]. Consequently, there is a pressing need for accessible, non-pharmacological therapeutic solutions that can be used both in clinical settings and at home to support personalized rehabilitation and continuous management of MSK pain.

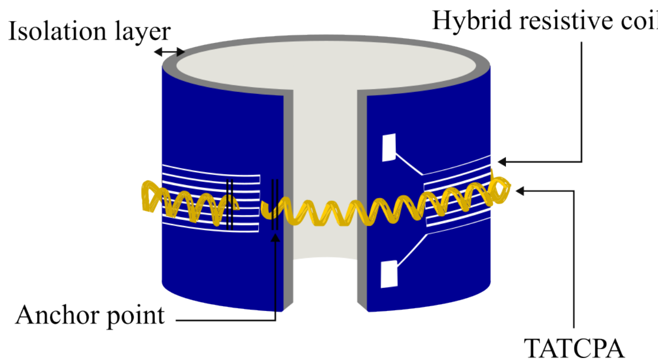

Fig. 1. Schematic view of the multimodal band illustrating the main components.

Manual therapy, physiotherapeutic exercise, and thermal treatments are widely recognized as effective for managing MSK conditions [3], [4]. Heat therapy in particular plays a central role, providing pain relief, reducing stiffness and muscle spasms, and promoting local circulation [5]. Similarly, mechanotherapy, defined as the therapeutic use of mechanical stimulation to promote tissue repair or maintain homeostasis, has emerged as a cornerstone in rehabilitation medicine [6], [7]. By eliciting mechanotransduction responses at the cellular level, mechanical cues such as compression massage, or stretching can help modulate tissue regeneration, and inflammatory responses [8], [9].

In this context, wearable robotic systems and smart textile technologies offer a promising route to devise lightweight, and conformable mechanotherapeutic devices [10]. Current devices often rely on pneumatic or hydraulic actuation systems [11], [12]. Although these systems enable precise mechanical control, they are typically heavy, bulky, rigid, and cumbersome for daily or home-based therapy. Textile-based solutions would provide inherent advantages in terms of comfort, breathability, and ease of customization, essential features for home-based rehabilitation and personalized therapy [13]. Shape memory alloys (SMAs) and shape memory polymers (SMPs) have demonstrated the potential to provide compact, thermally-activated actuation [14], [15], [16]. Since they inherently couple thermal and mechanical actions, they are ideal candidates to develop a device capable of providing multimodal therapy.

In this work, we present the design of a fully textile-based armband module capable of delivering simultaneous

The work of L.C. was co-funded by the European Union (ERC, MUSE, G.A. 101116249). Views and opinions expressed are those of the authors only and do not necessarily reflect those of the European Union or the European Research Council. Neither the European Union nor the granting authority can be held responsible.

[1] The BioRobotics Institute and the Department of Excellence in Robotics and AI, Scuola Superiore Sant'Anna, Pisa, Italy (emails: leonardo.cappello@santannapisa.it, marco.lupi@santannapisa.it).
[2] Department of Technologies and Measurement, University of West Bohemia, Pilsen, Czechia (email: rsoukup@fel.zcu.cz).
[3] Department of Chemistry and Materials Science, Aalto University, Espoo, Finland (email: jaana.vapaavuori@aalto.fi).

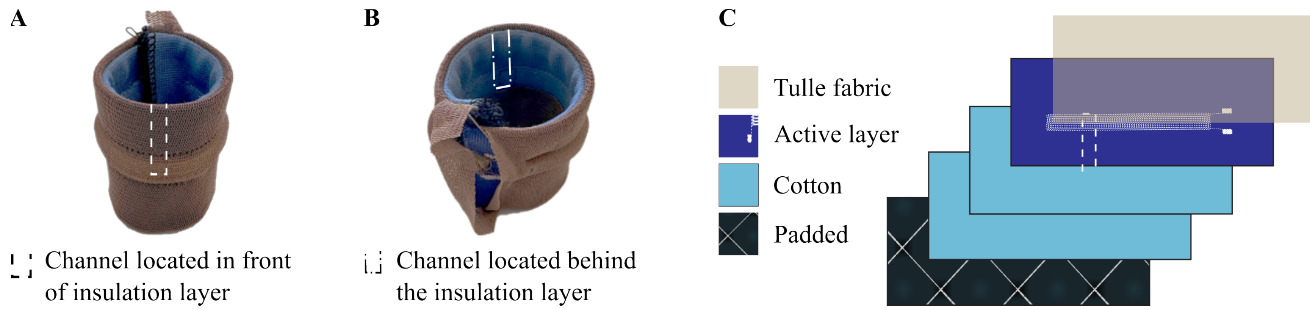

Fig. 2. (A) Front view and (B) back view of the multimodal textile band prototype. (C) Exploded schematic of the multilayer structure.

mechanical compression and thermal stimulation through the integration of thermally responsive fibres and embroidered resistive heating elements. Developed as a proof-of-concept, the prototype demonstrates the feasibility of a scalable, active multimodal device that combines mechanotherapy and heat therapy within a wearable textile platform, thus achieving a synergistic therapeutic effect.

II. DESIGN

The proposed system combines thermal and programmable mechanical actuation within a textile architecture by exploiting thermally activated polymer fibres together with a resistive heating coil. In particular, we adopted thermally activated twisted and coiled polymer actuators (TATCPAs) fabricated by The Multifunctional Materials Design research group (MMD) at Aalto University, through proprietary manufacturing techniques. These fibres exhibit reversible bending upon localized thermal activation. In parallel, hybrid resistive heating elements were designed and produced by Research and Innovation Centre for Electrical Engineering (RICE) at University of West Bohemia, using textile-based fabrication methods to integrate electronic components directly into the fabric. At the Textile Robotics Lab, Scuola Superiore Sant'Anna, we designed and integrated the prototype that consists of a tight-fitting textile band designed to apply cyclic compression to a targeted body region. The active fibres are arranged circumferentially along the band, positioned above the resistive heating coils. In the initial state, prior to thermal activation, the band applies a compressive load to the underlying tissue. As the resistive elements heat up, the TATCPAs undergo uniform thermal deformation, causing the band to expand and thereby reducing the applied pressure. The combination of two fibres and a resistive heating coil builds the active unit. This unit is approximately $1.0\,\mathrm{cm}$ wide, corresponding to the diameter of the TATCPAs ($0.4\,\mathrm{cm}$ each) plus a $0.1-0.2\,\mathrm{cm}$ spacing to allow independent fibre expansion and avoid mutual interference that could limit deformation. To protect the user's skin and ensure efficient heat transfer, a cotton-padded insulation layer is inserted between the heating coils and the skin. This layer serves a dual function: it prevents direct exposure to the high temperatures required for TATCPA activation, and it acts as a thermal buffer during the cooling phase, providing a prolonged therapeutic thermal effect. Combined with the compression–release cycle, this controlled thermal environment supports musculoskeletal recovery while promoting vascular and lymphatic circulation. The system is entirely powered and controlled by an Arduino UNO, with a PID controller that exploits real-time temperature feedback to modulate the supplied power and maintain the desired thermal profile, ensuring compactness and portability. Two textile-embedded channels were sewn respectively in front of and behind the insulation layer. These channels enable the stable positioning of NTC temperature sensors for continuous thermal monitoring. One sensor remains in direct contact with the heating resistor, while the other measures the temperature on the outer surface of the band, i.e., at the skin interface. Finally, a thin tulle fabric forms the outermost layer of the band, acting as a guiding channel to direct the TATCPA fibre deformation and facilitate controlled expansion of the band. This layer is sewn onto the fabric integrating the embroidered heating elements, fixed around the embroidery for the positioning of the fibres, as shown in Fig. 1 and Fig. 2. Each actuator is housed within its own dedicated channel to prevent mechanical interference between neighboring fibres during activation, as the helical expansion could otherwise be obstructed. The channels are designed with sufficient clearance between the fibre and the stitching to avoid friction or snagging during motion, ensuring reliable and repeatable actuation performance.

A. *TATCPA fibre*

Mechanical actuation in the proposed device is provided by twisted-and-coiled polymer actuators (TATCPAs) fabricated from Kinetic Super Mono ultra-high-molecular-weight polyethylene (UHMWPE) fishing line [17]. In general, their activation temperature and actuation behavior depend on both intrinsic material parameters - such as molecular weight, melting point, and degree of crystallinity - and fabrication parameters, including the diameter of the filaments, the one of the coil, and thermosetting conditions [18], [19]. The spring index (ratio of coil diameter to filament thickness) strongly affects actuation: thinner filaments and larger spring indices yield greater displacements, whereas thicker filaments and smaller spring indices increase load capacity. Twisting and coiling pre-stress the fibre, providing the internal stress required for actuation. The actuators employed in this study, first proposed and characterized in [17], [18], are made from single-ply filaments (0.4 cm diameter), fabricated from Kinetic Super Mono ultra-high-molecular-weight polyethylene (UHMWPE) fishing line. Filaments were coiled around 0.2 cm mandrels under constant tension to introduce internal stress. Coils were then thermoset at 192 °C for 150 minutes in a hydrothermal oven to stabilize their helical geometry and confer shape-memory properties. After cooling, they were removed from the mandrels and integrated into the textile band (Fig. 3).

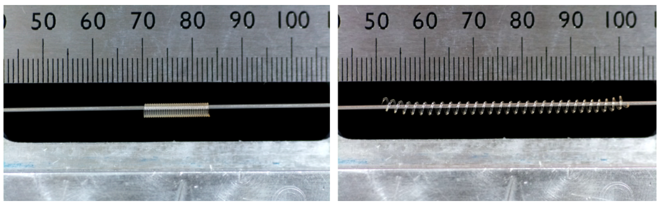

Fig. 3. Images of a twisted-and-coiled polymer actuator (TATCPA) in its initial relaxed state (at 25 °C) and expanded heated state (heated over its activation temperature)

B. Resistive Heating Elements

Hybrid conductive threads combine a textile filament core with embedded metallic microwires (see Fig. 4). The textile component provides a familiar feel as well as mechanical properties comparable to standard fibres, which enables straightforward integration into conventional textile technologies (e.g., embroidery, knitting, or weaving). In contrast, the metallic microwires impart electrical conductivity and mechanical robustness, ensuring high durability even under repeated automated washing [20], [21]. The specific thread used in this study, Clevertex No. 53, consists of a polyester filament combined with four non-insulated silver-plated copper microwires with a diameter of $30\,\mu\mathrm{m}$ and an electrical resistance of $6,5\,\Omega/\mathrm{m}$. The thread is also health-safe in accordance with Regulation (EC) No. 1907/2006 (REACH). The embroidery process was carried out on a Bernina embroidery machine, using Clevertex No. 53 as the upper thread and standard non-conductive polyester as the bobbin thread. Hot spots and enhances the safety of the heater, since the textile substrate provides both a thermal buffer and mechanical flexibility. Convection and radiation still contribute to the overall heat dissipation, but to a lesser extent compared to conduction, which remains the dominant pathway in textile-based heaters.

C. Insulation Layer

One challenge in this design prototype is to effectively insulate the heated elements from the human skin without compromising on the temperature needed for actuation and therapeutic stimulation. Therefore, it is critical to: (i) maintain 70 °C degrees on one part of the band to actuate the fibre, but (ii) not exceed 48 °C on the surface in direct contact with the wearer's skin to shield it from this actuation temperature, and to (iii) sustain a warm contact surface temperature to facilitate and prolong the therapeutic heating effect. To find the optimal textile layering for such insulation, ensuring user

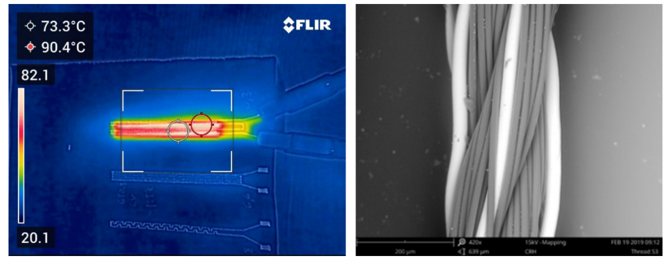

Fig. 4. Thermal response of the hybrid conductive threads (left). Close-up view illustrating the combination of metallic microwires and textile filaments within the thread structure (right).

safety while maintaining a stable therapeutic temperature, different materials and fabrics were explored and evaluated. By choosing these materials, a guiding aspect of this design is to find materials that feel natural to a wearer and are breathable and comfortable to wear. Under these premises, the following materials were tested:

(i) Single layer of interlock cotton knit
(ii) Double layer of interlock cotton knit
(iii) Double layer of interlock cotton knit + sandwiched foam sheet with cotton cover
(iv) Double layer of interlock cotton knit + padded polyester
(v) Foam sheet with cotton cover

For each configuration, temperature profiles were recorded over three heating–cooling cycles to evaluate thermal performance and repeatability. The safe skin-contact temperature for prolonged heat therapy, avoiding irritation, erythema, or burns, is considered to be approximately 42–43 °C. A higher threshold of 48 °C represents the limit that the skin can tolerate only for short exposure (on the order of seconds) [22].

III. RESULTS

A. Pressure test setup

To evaluate the pressure applied by the textile band, we 3D-printed a plastic cylinder (TPLA) with a diameter of 75 mm (approximately the diameter of the human arm [23]) and sensitized it with a 6-axis load cell (M3712A, SRI Sensor, China, see Fig. 5A,C). The band prototype was placed around the cylinder, and the compression force measured by the load cell was recorded, with an acquisition frequency equal to 100 Hz. Two commercial NTC thermistors were employed to monitor temperature at two critical locations. The first sensor was placed in contact with the heating coil, inserted in a channel sewn between it and the first insulation layer; the second one was placed into an external channel, sewn above the resistor outside of the insulation layer, the surface that would be in contact with the skin.

B. Preloading condition

The static preloading condition, representing the baseline compression applied by the band prior actuator activation, was characterized by computing the median of the compression force recorded for 30 s in the case of a single active fibre and in the one of two active fibres; the computed force

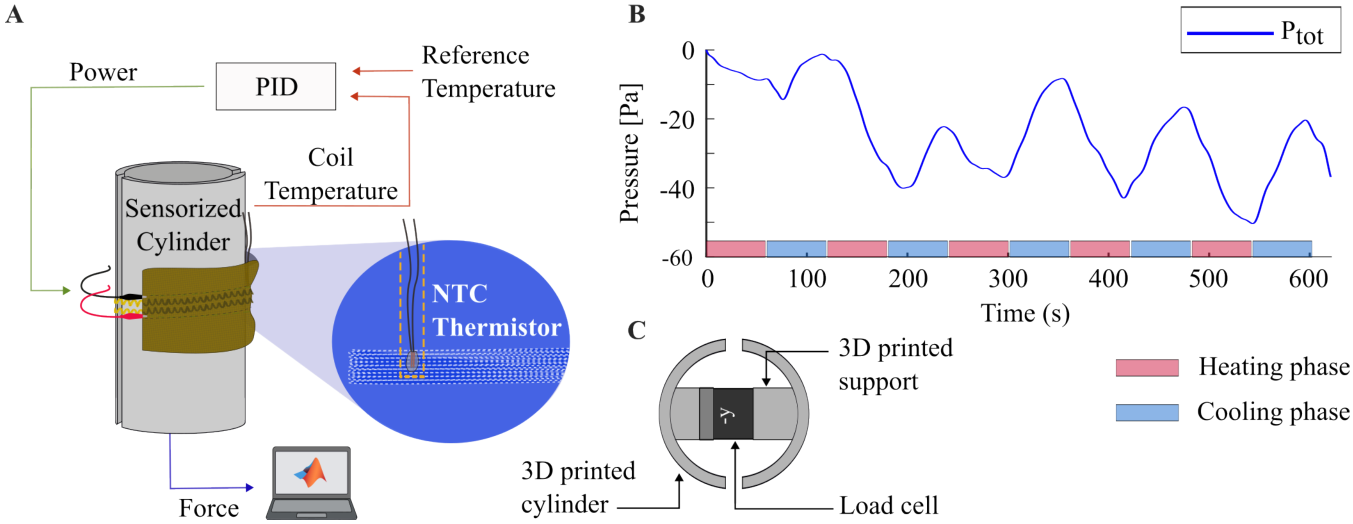

Fig. 5. (A) Experimental setup. The textile device is mounted on a sensorized cylindrical phantom used to measure the compression force exerted by the band. An NTC thermistor is inserted in a channel sewn between the heating coil and the first insulation layer. As shown in the zoomed view, the thermistor is positioned directly above the heating coil. The coil temperature serves as the feedback signal for a PID controller that regulates the electrical power supplied to the heating element. (B) Fluctuations of the total pressure result from the expansion and contraction of the active fibres during successive heating and cooling cycles. Negative values indicate a decrease in pressure with respect to the preload one. The pressure change is around $40\,\mathrm{Pa}$, with a marked baseline drift. (C) Section of the sensorized cylinder.

value was then divided by the estimated interface area of the band ($24\,\mathrm{cm}^2$) to obtain a measure of the initial pressure exerted by the active area of the device. In the configuration with one active fibres we obtained a median static pressure of $47.7\,\mathrm{Pa}$, with an interquartile range (IQR) of $4.67\,\mathrm{Pa}$, while two active fibres led to a median static pressure of $88.1\,\mathrm{Pa}$ with an IQR of $6.91\,\mathrm{Pa}$.

C. Heating cycle test

The band prototype, embedded with two fibres, was subjected to cyclic heating–cooling for 10 minutes to evaluate the pressure variation during a simulated therapy session. Temperature feedback from the NTC thermistor placed in contact with the heating coil was employed by a PID controller to regulate the power supplied to the coil, ensuring that the active fibres reached and maintained the target activation temperature of $70\,^{\circ}\mathrm{C}$ during the heating phase. The controller parameters were empirically set to

$$K_p = 5\,\frac{\mathrm{W}}{{}^{\circ}\mathrm{C}}, \quad K_i = 0.05\,\frac{\mathrm{W}}{s{}^{\circ}\mathrm{C}}, \quad K_d = 0.005\,\frac{\mathrm{Ws}}{{}^{\circ}\mathrm{C}}.$$

Each thermal cycle lasted $120\,\mathrm{s}$, divided into a $60\,\mathrm{s}$ heating phase followed by a $60\,\mathrm{s}$ cooling phase, for a total of five consecutive cycles ($10\,\mathrm{min}$ of device use). The pressure profile recorded by the load cell exhibits oscillations (Fig. 5B). During the first heating cycle, an initial preconditioning phase is observed, after which subsequent cycles show a stabilized elongation behavior, corresponding to a pressure variation of approximately $40\,\mathrm{Pa}$. To better highlight pressure fluctuations, the offset given by the static preload was subtracted from the recorded force, with negative values indicating a decrease in pressure with respect to the preload one. Pressure changes exhibited a time delay with respect to temperature variations, estimated to be $5.13\,\mathrm{s}$ in the heating phase and $13.31\,\mathrm{s}$ in the cooling phase. These asymmetries, caused by differences in temperature-pressure response between phases, are attributable to the intrinsic thermo-mechanical dynamics of the active fibres, which is markedly nonlinear [17], and of textiles in general. The pressure profile also exhibits a marked drift ($10\,\mathrm{Pa}$) in the baseline, due to the prolonged time interval as well as the hysteresis associated to the mechanical behavior of both fabric substrate and fibres.

D. Temperature Characterization of the Insulation Layer

Different textile configurations were investigated to identify an insulation architecture capable of ensuring user safety while maintaining a sustained therapeutic temperature. The safe temperature range for prolonged heat therapy is reported to be between $42\,^{\circ}\mathrm{C}$ and $43\,^{\circ}\mathrm{C}$, which prevents skin irritation or burns, whereas $48\,^{\circ}\mathrm{C}$ represents the upper limit tolerable only for short exposure durations. Five insulation configurations were evaluated (Fig. 6): (i) single layer of interlock cotton knit, (ii) double cotton jersey layer, (iii) foam sheet with cotton cover, (iv) double layer of interlock cotton knit + sandwiched foam sheet with cotton cover, and (v) double layer of interlock cotton knit + padded polyester. The configurations were selected to balance insulation performance with minimal bulk. Starting with a single layer of cotton ($< 1\,\mathrm{mm}$), additional layers were added to improve performance. Foam and padded polyester layers were tested for their ability to trap air and improve insulation, with thicknesses approximately of $2\,\mathrm{mm}$ and $4\,\mathrm{mm}$. Each configuration underwent three consecutive heating–cooling cycles and the surface temperature was monitored through the NTC thermistor positioned on the external side of the insulation layer. During the heating phase, the power supplied to the heating coil was regulated by the PID controller, ensuring that it reached the activation temperature of the fibres. During

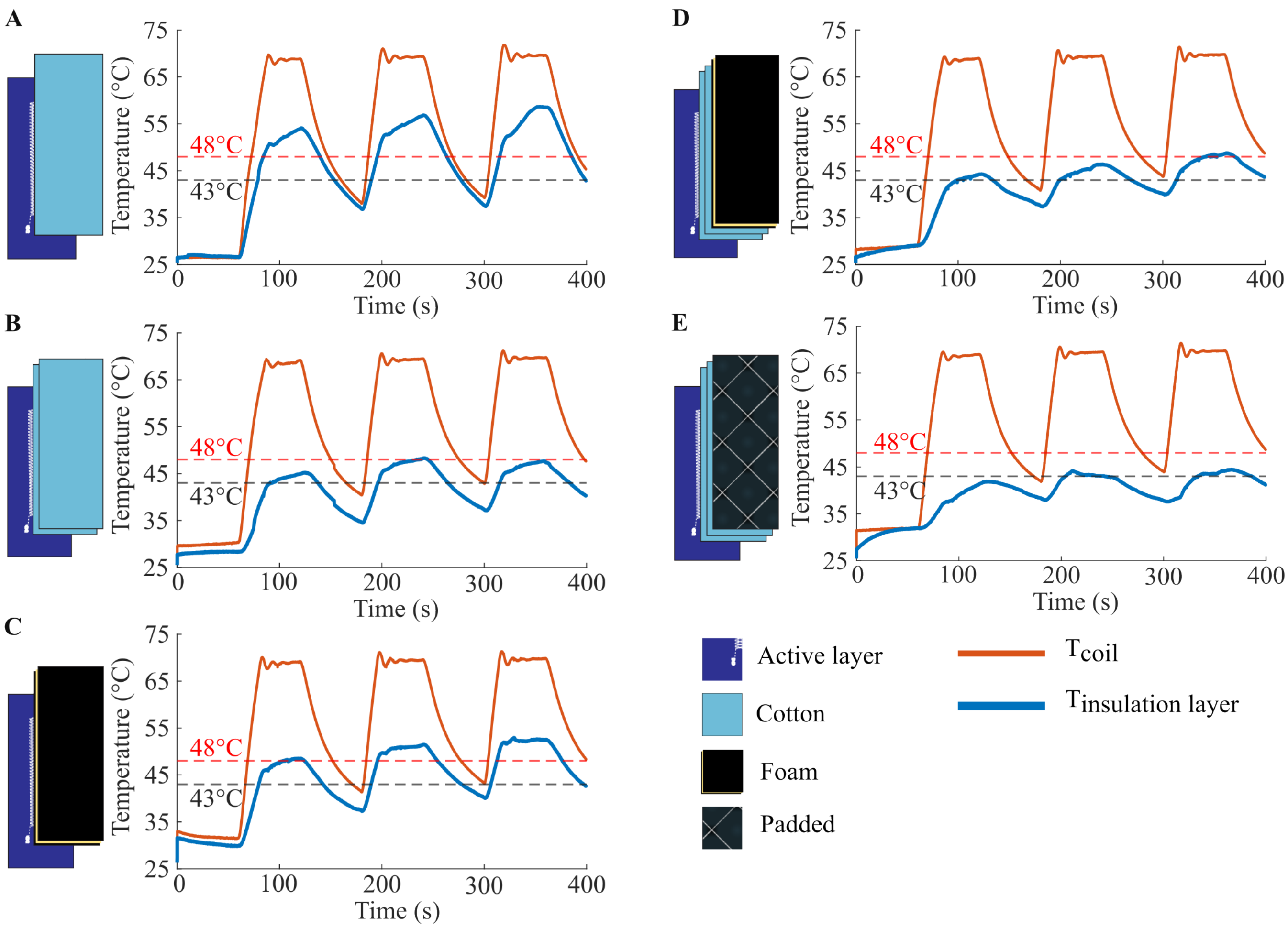

Fig. 6. Temperature profiles for five different insulation configurations: (A) single cotton layer, (B) double cotton layer, (C) black cotton combined with foam, (D) double cotton layer combined with black cotton and foam, and (E) double cotton layer combined with a polyester padded layer. The orange curves represent the temperature of the heating coil over three consecutive heating–cooling cycles. The coil reached the target temperature of 70 °C within 10–15 s and maintained a steady state for approximately 45–50 s. During the cooling phase, the system was switched off for 60 s. The blue curves indicate the temperature measured at the external surface of the insulation layer. The critical temperature thresholds of 43 °C and 48 °C are highlighted by dashed lines. Configuration (v) did not exceed the safety limits during the test and exhibited limited heat dispersion, ensuring a sustained thermal effect.

the cooling phase, the controller stopped supplying power to the coil for 60 s. Fig. 6 illustrates the temperature profiles for the different configurations, highlighting their respective thermal insulation performances.

IV. Discussion

The experimental results confirm the feasibility of a fully textile-based platform integrating programmable compression and localized heating within a single multimodal module. The applied pressure scaled proportionally with the number of active TATCPAs: doubling the number of actuators nearly doubled the preload pressure, suggesting the potential of parallel fibres arrangements in modular architectures to increase force output. Moreover, serial configurations can extend band deformation and dynamic pressure change. Despite the low absolute pressures (below $0.1\,\mathrm{kPa}$), significantly lower than the therapeutic pressure range of $2-10\,\mathrm{kPa}$ typically reported for vascular and lymphatic therapies [10], these values are consistent with the limited $1\,\mathrm{cm}$ active section of each unit (heating coil + two fibres). Given the compact dimensions of the actuation module, achieving clinically relevant compression levels would require the integration of several tens of units. Nevertheless, this modular configuration would still result in a wearable device with an estimated length of approximately $20-30\,\mathrm{cm}$. To further validate these findings, a theoretical model of the system will be developed to assess the feasibility of the parallelization strategy. Finally, thermal characterization demonstrated effective spatial separation between actuation and skin-contact regions. This effect can be attributed to the low thermal conductivity of the selected textile materials and to the air retained within the fibrous architecture. Cotton typically exhibits thermal conductivity values in the range of $0.04-0.06\,\mathrm{W/mK}$, while polyester fibres show comparable or slightly lower values ($0.03-0.05\,\mathrm{W/mK}$) [24]. However, the main contribution arises from trapped air ($\sim\ 0.026\,\mathrm{W/mK}$) in padded or foam layers, which significantly increases the effective thermal resistance of the multilayer architecture [25]. With the selected multilayer insulation - comprising double cotton layers and polyester padding - the actuator side reached $70\,^{\circ}\mathrm{C}$, while the skin-side temperature remained within the therapeutic range of $42-44\,^{\circ}\mathrm{C}$ during heating. During the cooling phase, the external surface temperature decreased by only $\sim 6\,^{\circ}\mathrm{C}$ over $60\,\mathrm{s}$, ensuring a sustained and comfortable thermal effect. This concurrent delivery of controlled mechanical and thermal stimuli highlights the capability of the proposed textile design to provide safe, prolonged, and multimodal treatment suitable for wearable rehabilitation devices.

V. LIMITATIONS AND OUTLOOK

Given the very preliminary nature of this study, several limitations remain. Our prototype presented a significant drift during heating-cooling experiments, most likely due to the hysteretic behavior of complex structures such as textile materials. To address this issue, future work will investigate pre-conditioning heating-cooling cycles to reduce hysteresis, as well as a characterization of TATCPA fibres in terms of compressive force. The actuation system will be enhanced by testing multiple configurations that combine fibres in parallel or incorporate contractile fibres to optimize force delivery. Multi-zone actuation strategies will also be investigated to improve pressure distribution for different therapeutic protocols. Finally, fully textile-based temperature and strain sensors will be integrated to eliminate reliance on external instrumentation, and advanced control strategies could further enhance safety and prevent overheating. A hierarchical stack-of-tasks scheme could enforce temperature thresholds to prioritize patient safety, while predictive control may be implemented after detailed characterization of the device's thermal dynamics. Moreover, physiological factors such as sweat and moisture effects will be considered in future work. These factors can influence temperature dynamics and textile performance during long-term wearable use. These advancements will support the translation of textile-integrated multimodal rehabilitation devices into practical, home-based therapeutic applications.

VI. ACKNOWLEDGEMENTS

The authors thank Giada Ferti for her support in prototyping the integrated armband.

REFERENCES

[1] F. M. Blyth, A. M. Briggs, C. H. Schneider, D. G. Hoy, and L. M. March, "The global burden of musculoskeletal pain—where to from here?" *American Journal of Public Health*, vol. 109, pp. 35–40, 1 2019.

[2] T. Margham, "Musculoskeletal disorders: Time for joint action in primary care," pp. 657–658, 2011.

[3] R. Rossi, "Heat therapy for different knee diseases: expert opinion," 2024.

[4] T. Loghmani and M. Whitted, "Soft tissue manipulation: A powerful form of mechanotherapy," Tech. Rep., 2016.

[5] F. Nossa, M. Franco, A. Magni, E. Raimondo, G. Ventriglia, and F. Gervasoni, "Heat therapy for musculoskeletal pain conditions: Actionable suggestions for pharmacists from a panel of experts," *Pharmacy*, vol. 13, p. 63, 4 2025.

[6] C. Huang, J. Holfeld, W. Schaden, D. Orgill, and R. Ogawa, "Mechanotherapy: Revisiting physical therapy and recruiting mechanobiology for a new era in medicine," pp. 555–564, 9 2013.

[7] B. R. Seo and D. J. Mooney, "Recent and future strategies of mechanotherapy for tissue regenerative rehabilitation," pp. 4639–4642, 11 2022.

[8] X. Di, X. Gao, L. Peng, J. Ai, X. Jin, S. Qi, H. Li, K. Wang, and D. Luo, "Cellular mechanotransduction in health and diseases: from molecular mechanism to therapeutic targets," 12 2023.

[9] D. E. Ingber, "From tensegrity to human organs-on-chips: implications for mechanobiology and mechanotherapeutics," *Biochemical Journal*, vol. 480, pp. 243–257, 2 2023.

[10] T. Jiralerspong and H. Zhao, "Soft robotic devices for mechanotherapy of the upper and lower extremities," 5 2025.

[11] D. J. Preston, H. J. Jiang, V. Sanchez, P. Rothemund, J. Rawson, M. P. Nemitz, W.-K. Lee, Z. Suo, C. J. Walsh, and G. M. Whitesides, "A soft ring oscillator," Tech. Rep., 2019.

[12] R. Z. Gao, V. N. T. Mai, N. Levinski, J. M. Kormylo, R. W. Murdock, C. R. Dickerson, and C. L. Ren, "A novel air microfluidics-enabled soft robotic sleeve: Toward realizing innovative lymphedema treatment," *Biomicrofluidics*, vol. 16, 5 2022.

[13] A. Libanori, G. Chen, X. Zhao, Y. Zhou, and J. Chen, "Smart textiles for personalized healthcare," pp. 142–156, 3 2022.

[14] R. M. Granberry, J. M. Abel, and B. T. Holschuh, "Preliminary investigation of the design of a mechanically antagonistic, actuating countermeasure garment," Tech. Rep., 2020.

[15] H. Narayana, J. Hu, B. Kumar, S. Shang, M. Ying, and R. J. Young, "Designing of advanced smart medical stocking using stress-memory polymeric filaments for pressure control and massaging," *Materials Science and Engineering C*, vol. 91, pp. 263–273, 10 2018.

[16] R. Granberry, M. Clarke, R. Pettys-Baker, H. Woelfle, C. Compton, A. Ross, K. Johnson, S. Padula, S. Shah, J. Abel, and B. Holschuh, "Dynamic, tunable, and conformal wearable compression using active textiles," *Advanced Materials Technologies*, vol. 7, 12 2022.

[17] Z. Madani, P. E. Silva, H. Baniasadi, M. Vaara, S. Das, J. C. Arias, J. Seppälä, Z. Sun, and J. Vapaavuori, "Light-driven multidirectional bending in artificial muscles," *Advanced Materials*, vol. 36, 9 2024.

[18] Y. Zhang, M. Vaara, A. Alesafar, D. B. Nguyen, P. Silva, L. Koskelo, J. Ristolainen, M. Stosiek, J. Löfgren, J. Vapaavuori, and P. Rinke, "Data-efficient optimization of thermally-activated polymer actuators through machine learning," *Materials and Design*, vol. 253, 5 2025.

[19] C. S. Haines, M. D. Lima, N. Li, G. M. Spinks, J. Foroughi, J. D. Madden, S. H. Kim, S. Fang, M. Jung de Andrade, F. Göktepe *et al.*, "Artificial muscles from fishing line and sewing thread," *science*, vol. 343, no. 6173, pp. 868–872, 2014.

[20] C. Dils, D. Kalas, J. Reboun, S. Suchy, R. Soukup, D. Moravcova, M. von Krshiwoblozki, and M. Schneider-Ramelow, "Interconnecting embroidered hybrid conductive yarns by ultrasonic plastic welding for e-textiles," pp. 4501–4520, 11 2022.

[21] R. Polanský, R. Soukup, J. Řeboun, J. Kalčík, D. Moravcová, L. Kupka, M. Švantner, P. Honnerová, and A. Hamáček, "A novel large-area embroidered temperature sensor based on an innovative hybrid resistive thread," *Sensors and Actuators, A: Physical*, vol. 265, pp. 111–119, 10 2017.

[22] M. W. Dewhirst, B. L. Viglianti, M. Lora-Michiels, M. Hanson, and P. J. Hoopes, "Basic principles of thermal dosimetry and thermal thresholds for tissue damage from hyperthermia," in *International Journal of Hyperthermia*, vol. 19, 5 2003, pp. 267–294.

[23] A. M. Tang, M. Chung, K. R. Dong, P. Bahwere, K. Bose, R. Chakraborty, K. Charlton, P. Das, M. Ghosh, M. I. Hossain, P. Nguyen, C. B. Patsche, T. Sultana, M. Deitchler, and Z. Maalouf-Manasseh, "Determining a global mid-upper arm circumference cut-off to assess underweight in adults (men and non-pregnant women)," *Public Health Nutrition*, vol. 23, pp. 3104–3113, 12 2020.

[24] S. B. Stanković, D. Popović, and G. B. Poparić, "Thermal properties of textile fabrics made of natural and regenerated cellulose fibers," *Polymer testing*, vol. 27, no. 1, pp. 41–48, 2008.

[25] J. Nadzeikienė, R. Milašius, J. Deikus, J. Eičinas, and P. Kerpauskas, "Evaluating thermal insulation properties of garment packet air inter-layer," *Fibres & Textiles in Eastern Europe*, vol. 14, no. 1 (55), 2006.